CCFE-PR(15)85

Z.S. Qu, M.J. Hole and M. Fitzgerald

Energetic geodesic acoustic modes associated with two-stream like instabilities in tokamak plasmas

Energetic geodesic acoustic modes associated with two-stream like instabilities in tokamak plasmas

Z.S. Qu[1], M.J. Hole[1] and M. Fitzgerald[2]

[1]Research School of Physics and Engineering, the Australian National University, Canberra, ACT, 2601, Australia
[2]CCFE Fusion Association, Culham Science Centre, Abingdon, Oxon, OX14 3DB, UK

Energetic geodesic acoustic modes associated with two-stream like instabilities in tokamak plasmas

Z.S. Qu and M.J. Hole

Research School of Physics and Engineering,

the Australian National University, Canberra ACT 2601, Australia

M. Fitzgerald

CCFE Fusion Association, Culham Science Centre, Abingdon, Oxon, OX14 3DB, UK

Abstract

An unstable branch of energetic geodesic acoustic mode (EGAM) is found using the fluid theory with fast ions characterised by their narrow width in energy distribution and collective transit along field lines. This mode, with a frequency much lower than the thermal GAM frequency $\omega_{\rm GAM}$, is now confirmed as a new type of unstable EGAM : a reactive instability similar to the two-stream instability. The mode can have very small fast ion density threshold when the fast ion transit frequency is smaller than $\omega_{\rm GAM}$, consistent with the on-set of the mode right after the turn-on of the beam in DIII-D experiments. The transition of this reactive EGAM to the velocity gradient driven EGAM is also discussed.

Recent experiments [1–3] with neutral beam injection show bursting $n = 0$ axisymmetic modes at half of the thermal geodesic acoustic mode (GAM) [4, 5] frequency, which are identified as the energetic-particle-induced GAMs (EGAMs). The presence of EGAMs are found responsible for fast ion losses [6] and may enhance turbulence transport, leading to the destruction of internal transport barriers [7] and the degradation of fusion confinement. Many efforts have been made to model [8–12] and simulate [13–16] EGAMs both linearly and nonlinearly using a kinetic or hybrid-kinetic theory. One of the major outcomes is the discovery of multiple branches of GAMs in the presence of fast particles. The lower frequency branch is excited by the inverse Landau damping provided by the fast ions. In tokamaks, most of these works assume a fast ion distribution with a large width in energy (e.g. the slowing down distribution function). However, the magnetic spectrogram in DIII-D experiments [1] showed a turn-on of the mode $1ms$ right after the beam switched on, much faster than the beam slowing down time($\sim$ tens of ms), indicating that the beam ions are not slowed down when the mode first appears. Also, due to the limited width in energy distribution, the beam may not provide sufficient inverse Landau damping to enable the growth of the mode. One possible explanation is proposed by Berk *et al* [9], in which the early EGAMs are negative energy modes, the presence of whom will reduce the total energy of the system. They are driven unstable by thermal ion Landau damping.

Due to its simplicity and intuitive nature, the fluid theory, if its regime of validity is properly considered, may shed lights on the underlying physics which may otherwise be confused with wave-particle interaction physics. By using a fluid description of the fast ions, we have found a new class of unstable EGAMs associated with beam ions. These EGAMs are similar to the two stream instabilities rather than driven by the inverse Landau damping. They have a high growth rate ($\sim 30\%$ mode frequency) which increases steeply as fast ion density increases, consistent with the early turn-on of the mode.

We consider a tokamak plasma with large aspect ratio, circular cross section and low β. The flux surfaces are concentric and labeled by radial coordinate r, while θ and φ give the poloidal and toroidal angle, respectively. In this work, we adopt a local treatment, making $\rho_s < q\rho_s \ll L_{\rm EGAM}$ where $L_{\rm EGAM}$ is the width of the mode, ρ_s the Larmor radius and $q\rho_s$ gives approximately the drift orbit width. The change of equilibrium quantities in radial direction is ignored. We assume that the plasma consists of thermal and fast ions, all with mass m_i and unity charge e, as well as electrons with negligible inertia and negative charge

$-e$. Thermal ions have density n_i and temperature T_i, while for fast ions, the density n_f, the parallel pressure $p_{\parallel f}$ and the perpendicular pressure $p_{\perp f}$ are obtained by integrals of the fast ion guiding center distribution. The thermal ions are static with $V_i = 0$. The fast ions have an average transit speed V_f along the field lines.

The dynamic of the system is determined by the linearized momentum equation of each species "s", given by

$$m_s n_s \left(\frac{\partial \tilde{\boldsymbol{V}}_s}{\partial t} + \frac{\tilde{n}_s}{n_s} \boldsymbol{V}_s \cdot \nabla \boldsymbol{V}_s + \boldsymbol{V}_s \cdot \nabla \tilde{\boldsymbol{V}}_s + \tilde{\boldsymbol{V}}_s \cdot \nabla \boldsymbol{V}_s \right) = n_s q_s (-\nabla \tilde{\Phi} + \tilde{\boldsymbol{V}}_s \times \boldsymbol{B}) - \nabla \cdot \tilde{\overline{P}}, \tag{1}$$

in which q_s is the charge, $\tilde{\Phi}$ the perturbed electrostatic potential, $\tilde{\overline{P}} = \tilde{p_\perp} \overline{I} + (\tilde{p_\parallel} - \tilde{p_\perp}) \boldsymbol{bb}$ the perturbed pressure tensor, with $\boldsymbol{b} = \boldsymbol{B}/B$ and $\boldsymbol{B}$ the magnetic field. The subscript "s" labels electrons (e), thermal ions (i) or fast ions (f) and the circumflex labels the perturbed quantities. The perturbed velocity consists of the perpendicular and parallel components, written as

$$\tilde{\boldsymbol{V}}_s = \tilde{\boldsymbol{V}}_E + [\tilde{V}_{s+}(r) e^{i\theta} + \tilde{V}_{s-}(r) e^{-i\theta}] \boldsymbol{b}, \tag{2}$$

where $\tilde{\boldsymbol{V}}_E$ is the $\boldsymbol{E} \times \boldsymbol{B}$ drift velocity. Considering the small orbit width assumption, we only retain $m = 0$ component of $\tilde{\Phi}$ for the $\boldsymbol{E} \times \boldsymbol{B}$ drift and $m = \pm 1$ components of parallel velocity that are lowest order in $q\rho_s$, while the magnetic gradient/curvature drifts are higher order terms and therefore ignored. Now $\tilde{\boldsymbol{V}}_E$ is in the direction of $\boldsymbol{\pi} = \boldsymbol{e}_r \times \boldsymbol{b}$. Similarly, the perturbed density and pressure are decomposed into $m = \pm 1$ harmonics, for instance, $\tilde{n}_i = \tilde{n}_{i+1} e^{i\theta} + \tilde{n}_{i-1} e^{-i\theta}$.

Adding up Eq. (1) for electrons, thermal and fast ions, ignoring electron inertia, imposing the quasi-neutrality condition $\nabla \cdot \tilde{\boldsymbol{J}} = 0$ ($\tilde{\boldsymbol{J}}$ is the perturbed current) and taking a flux surface average, we obtain the perpendicular momentum equation

$$\begin{aligned} m_i \langle n_0 \rangle \omega \tilde{V}_E = \frac{1}{2R} \sum_s [& \tilde{p_\perp}_{s+1} - \tilde{p_\perp}_{s-1} \\ & + \tilde{p_\parallel}_{s+1} - \tilde{p_\parallel}_{s-1} + m_s (\tilde{n}_{s+1} - \tilde{n}_{s-1}) \left\langle V_s^2 \right\rangle \\ & + 2 m_s \langle n_s V_s \rangle (\tilde{V}_{s+} - \tilde{V}_{s-})], \end{aligned} \tag{3}$$

where $n_0 = n_i + n_f$ is the total ion density and R is the major radius on axis, $\langle \ldots \rangle$ the flux surface average and ω the mode complex angular frequency ($\gamma = Im(\omega)$ gives the growth rate). We have used the identity

$$\nabla \cdot \boldsymbol{\pi} \approx -\boldsymbol{\pi} \cdot \nabla \ln B \approx (\boldsymbol{b} \cdot \nabla \boldsymbol{\pi}) \cdot \boldsymbol{b} = -\kappa_g \approx -\sin\theta / R, \tag{4}$$

which are all considered as geodesic curvature. The parallel momentum equations for thermal and fast ions are obtained from the parallel component of Eq. (1), with the potential terms canceled using the same equation for electrons, written as

$$m_i n_i \omega \tilde{V}_{i\pm} = \pm \frac{1}{qR} \left(\tilde{p_\parallel}_{i\pm 1} + \frac{n_i}{\langle n_0 \rangle} \tilde{p}_{e\pm 1} \right), \tag{5}$$

$$m_i n_f \left(\omega \mp \frac{\langle V_f \rangle}{qR} \right) \tilde{V}_{f\pm} = \pm \frac{1}{qR} \left(\tilde{p_\parallel}_{f\pm 1} + \frac{n_f}{\langle n_0 \rangle} \tilde{p}_{e\pm 1} \right) \pm \frac{m_i \langle V_f \rangle}{2R} \left\langle B \left(\frac{\partial n_f}{\partial B} \right)_r \right\rangle \tilde{V}_E, \tag{6}$$

where q is the safety factor.

The ion response to $\tilde{\boldsymbol{V}}_E$ is described by the Chew-Goldberger-Low (CGL) law [17], assuming that the ion perpendicular and parallel pressure are doing work independently. An agreement is reached between the CGL and the gyrokinetic theory on the thermal GAM frequency [18, 19]. It has also been shown that when the mode frequency is much higher than the thermal frequency of the bulk ions (in conventional GAM, $q \gg 1$) the CGL law can give a good description of the plasma response [20, 21]. This CGL law is given by

$$\frac{dp_{\parallel s}}{dt} = -p_{\parallel s} \nabla \cdot \boldsymbol{V}_s - 2 p_{\parallel s} \boldsymbol{b} \cdot (\boldsymbol{b} \cdot \boldsymbol{V}_s), \tag{7}$$

$$\frac{dp_{\perp s}}{dt} = -2 p_{\perp s} \nabla \cdot \boldsymbol{V}_s + p_{\perp s} \boldsymbol{b} \cdot (\boldsymbol{b} \cdot \boldsymbol{V}_s). \tag{8}$$

The response of electrons is assumed to be isothermal,which means

$$\tilde{p}_e = \tilde{n}_e T_e = (\tilde{n}_i + \tilde{n}_f) T_e, \tag{9}$$

from the quasi-neutrality condition, while $\tilde{n}_i$ and $\tilde{n}_f$ are obtained from the ion continuity equation given by

$$\frac{\partial \tilde{n}_s}{\partial t} = -\nabla \cdot (n_s \tilde{\boldsymbol{V}}_s + \tilde{n}_s \boldsymbol{V}_s). \tag{10}$$

We can simplify Eq. (7), (8) and (10) using Eq. (4), giving the relationship between the perturbed pressure and perturbed velocity. These equations, along with Eq. (9), close the system and define the dispersion relationship $D(\omega) = 0$. In the $q \gg 1$ limit where the coupling to the thermal ion sound wave is ignored, $D(\omega)$ is given by

$$D(\omega) = 1 - (1 - \alpha) \frac{\omega^2_{\mathrm{GAM}}}{\omega^2} - \alpha G(\omega), \tag{11}$$

where $\omega^2_{\mathrm{GAM}} = \frac{2T_i}{m_i R^2} \left(\frac{7}{4} + \frac{T_e}{T_i} + O(\frac{1}{q^2}) \right)$ is the square of the thermal GAM frequency and $\alpha \equiv \langle n_f \rangle / n_0$ is the fast population fraction. The exact form of $G(\omega)$ depends on the fast ion

distribution function, but since the fluid theory has ignored Landau Damping effects, $G(\omega)$ is real if $Im(\omega) = 0$.

We first consider a bump-on-tail distribution function given by

$$F(v_\parallel, v_\perp) = n_f A \exp\left[-\frac{m(v_\parallel - V_f)^2 + m v_\perp^2}{2T_f}\right], \tag{12}$$

where A is a normalization factor, $v_\parallel$ and $v_\perp$ are parallel and perpendicular velocity, respectively. For small α and negligible energy width T_f, $G(\omega)$ is given by

$$G(\omega) \approx \frac{\frac{3}{2}\omega_b^2 q^2}{\omega^2 - \omega_b^2} + \frac{\omega_b^4 q^2}{(\omega^2 - \omega_b^2)^2}, \tag{13}$$

where $\omega_b \equiv V_f/qR$ is the average fast ion transit frequency. The dispersion relationship now becomes a cubic equation of ω^2 with three solutions. Properties of the solutions are determined by the relationship between $\omega_{\rm GAM}$ and ω_b, as well as q and the fast ion population.

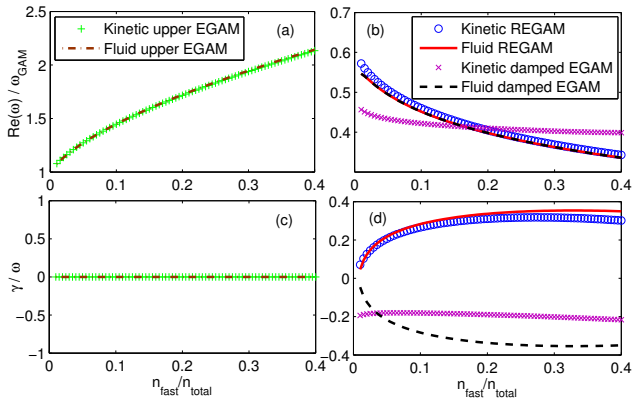

FIG. 1. Real frequency (a)(b) and growth rate (c)(d) versus fast ion density for multi-fluid model with comparison to kinetic theory, for $q = 4$ and $\omega_b = 0.58\omega_{\rm GAM}$. Lines/symbols: fluid/kinetic results.

In FIG.1, we plot the solutions to ω with parameters $q = 4$ and $\omega_b = 0.58\omega_{\rm GAM}$, retaining finite energy width $T_f = 0.25T_i$, for fast particle concentration from 1% to 40%. Similar to Fu *et al* , multiple branches of GAMs are presented. The frequency of the upper (frequency) EGAM, as seen in FIG.1 (a), increases with increasing fast particle population. This branch reduces to the thermal GAM when $n_f = 0$. We compare our fluid result to the numerical solution of the kinetic dispersion relationship [16, 22], showing very good agreement. In this case, the Landau damping from the thermal particles is negligibly small. Also, two complex conjugated branches are presented in FIG.1 (b) and (d) at lower frequency, both having

decreasing frequency with higher fast ion fraction. We note that the existence of these branches is due to the Doppler shift of the wave in the static frame of the fast ions, since this is the only effect of the fast ion when T_f is small. One of these modes is found unstable in kinetic theory, and is previously attributed to the inverse Landau damping. However, the same growth rate is also obtained using the fluid model. Given that no Landau damping is presented in the fluid theory, this instability cannot come from the wave-particle interaction, but must be a reactive instability. This conclusion is strengthened by the observation that the mode remains unstable even when it enters in the region with $\partial F/\partial E < 0$ for $\alpha > 0.27$. We name this unstable branch the Reactive EGAM (REGAM) from its nature of instability. By solving the dispersion relationship Eq. (11) and (13), we obtain the growth rate for $\alpha \ll 1$, given by

$$\gamma \approx \frac{1}{2} q \omega_b^2 (\omega_{\rm GAM}^2 - \omega_b^2)^{-\frac{1}{2}} \sqrt{\alpha}, \tag{14}$$

with no fast ion density threshold. Finally, we find that the fluid theory is valid for the upper EGAM and the REGAM, which are on the real axis or the upper plane, while the other damped EGAM is located on the lower plane and is strongly modified by Landau damping, leading to the deviation of its fluid solution from the kinetic theory.

For the regime $\omega_b > \omega_{\rm GAM}$, the upper EGAM will start at ω_b instead of the thermal GAM frequency, as shown in FIG.2 (a) with parameters $T_f = T_i$, $q = 2$ and $\omega_b = 1.76\omega_{\rm GAM}$. The kinetic theory gives a finite Landau damping rate, while in the fluid theory, this mode is predicted to be stable. One of the lower modes starts at $\omega_{\rm GAM}$ when $n_f = 0$. Unlike FIG.1, the lower modes have an instability threshold of $\alpha > 0.05$. In FIG.2 (b) and (d), the unstable REGAM and a damped EGAM occur between $0.05 < \alpha < 0.25$ when the two modes have the same real frequency. This real frequency bifurcates at $\alpha = 0.25$, with the modes become stable at the same time. Parameter scan shows that the bifurcation point moves to lower α value when ω_b increases. For $\omega_b > 2\omega_{\rm GAM}$, no unstable mode is presented. Again, FIG.2 shows a good match to the kinetic theory.

The origin of the instability can be studied by calculating the wave energy of the two lower frequency modes. In FIG.2 (b) when $\alpha > 0.25$, the lower frequency mode is a positive energy wave ($dD(\omega)/d\omega > 0$) while the other is a negative energy one ($dD(\omega)/d\omega < 0$). The strong coupling of these two modes is achieved when they possess the same real frequency ($0.05 < \alpha < 0.25$), where the REGAM occurs. The energy can transfer from the negative energy wave to the positive energy wave, enabling the growth of both modes meanwhile

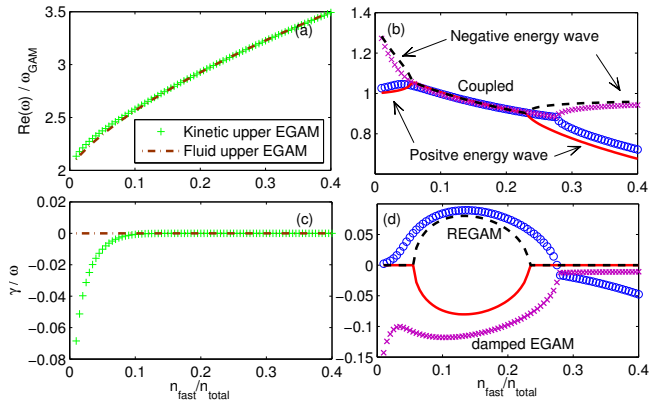

FIG. 2. Real frequency (a)(b) and growth rate (c)(d) versus fast ion density for multi-fluid model with comparison to kinetic theory, for $q = 2$ and $\omega_b = 1.76\omega_{\rm GAM}$. Lines/symbols: fluid/kinetic results.

conserving the total energy [23]. Therefore, this GAM instability shares great similarities to the two-stream instabilities in a beam plasma system, which can also be captured by a fluid model.

We now apply our results to the early turn-on of EGAMs in DIII-D by considering a single energy single pitch beam distribution function, before the slowing down or pitch angle scattering can happen. This distribution function is given by

$$F(E,\Lambda) = \frac{n_f}{2\pi v_\perp}\delta(E-E_0)\delta(\Lambda-\Lambda_0), \tag{15}$$

where E is the fast ion energy, Λ the pitch angle and $\delta(x)$ the Dirac delta function. The form of $G(\omega)$ is identical to Eq. (13) except the numerators now become a function of both E_0 and Λ_0. For the DIII-D beam in Nazikian *et al* [1], we have $E_0 = 75$keV and $\Lambda_0 = 0.5$. We also have $\omega_b = 0.88\omega_{\rm GAM}$ obtained from $T_e = 1.2T_i \approx 1.2$keV and $q = 4$ at the radial localized flux surface $s = 0.4$. Similarly we plot the real frequency and growth rate of the REGAM as a function of α in FIG.3 (the other two branches are damped and not discussed here). The frequency of the REGAM stays reasonably close to the observed frequency (28kHz) for $\alpha > 3\%$. Also, no density threshold is presented in the fluid theory, although in reality the background damping (such as collisional damping) may create a finite threshold. But since the growth rate is large and is a steep function of the fast ion density when the density is low ($\sim \sqrt{\alpha}$), this background damping can be overcome quickly as fast ion density increases, consistent with the early turn-on of the mode.

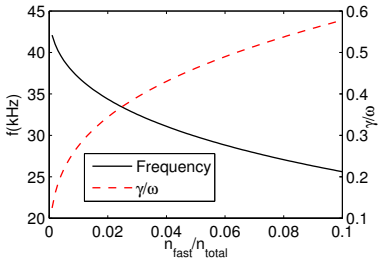

FIG. 3. Real frequency and growth rate of the REGAM using DIII-D parameters on flux surface $s = 0.4$.

Finally, we study the relationship between the REGAMs and the inverse Landau damping driven EGAMs (dissipative EGAMs). The unstable (R)EGAM frequency and growth rate versus the fast particle energy width T_f is plotted in FIG.4 for the bump on tail distribution. The parameters are identical to FIG.1. Figure 4 shows that the unstable EGAMs are reactive (REGAMs) for $T_f/T_i < 1$ where the fluid theory is valid, and dissipative for large T_f where the kinetic effects are dominant and the fluid treatment breaks down. A smooth transition is found in between these two regimes by solving the kinetic dispersion relationship [16, 22], indicating the natural conversion from the early turn-on REGAMs to the dissipative EGAMs, when the fast ions are slowed down in background plasma. Slowing down of the fast ions due to the nonlinear phase of REGAMs is also possible and requires further investigation.

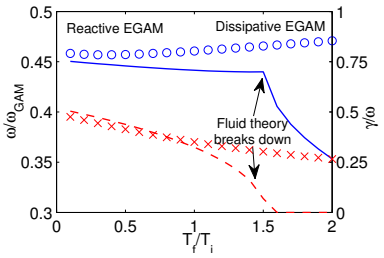

FIG. 4. Real frequency in fluid(blue solid line) and kinetic(blue circle) theory, and growth rate in fluid(red broken line) and kinetic(red cross) theory versus fast particle energy width T_f, for $n_f/n_0 = 0.1$, $q = 4$ and $\omega_b = 0.58\omega_{\rm GAM}$.

In summary, we have found a new unstable branch of EGAMs in the presence of beam ions with a small width in energy distribution, known as a reactive instability similar to the two-stream instability (REGAMs). This mode can have a much lower frequency than the thermal

GAMs and γ/ω up to 30% with no turn-on threshold when background damping is not considered. Our work shows that EGAM solutions are not inherent to kinetic approaches and one should not overlook the reactive contribution to the instabilities. We have demonstrated the consistency of REGAMs with the early turn-on of EGAMs in DIII-D experiments, a scenario that cannot be explained by the previous theories of inverse Landau damping driven EGAMs. We have also shown the possible smooth transition between these two types of EGAMs after the beam ions are slowed down. In addition, this work gives a good example of how the fluid theory can aid the understanding of fast particle physics. Further discussion about the region of validity of the fluid theory as well as the radial mode structure will be presented in following up publications.

The authors would like to thank Dr. A. Biancalani, Dr. G.Y. Fu, Prof. B.N. Breizman and Dr. B. Layden for fruitful discussions; Dr. M.A. Van Zeeland and Dr. R. Nazikian for DIII-D data. This work is funded by China Scholarship Council (ZSQ), the AINSE Postgraduate Research Award (ZSQ), Australian ARC project DP1093797 and FT0991899 (MJH). This work was part funded by the RCUK Energy Programme [grant number EP/I501045] (MF).

[1] R. Nazikian *et al.*, Phys. Rev. Lett. **101**, 185001 (2008).

[2] T. Ido *et al.*, Nucl. Fusion **51**, 073046 (2011).

[3] W. Chen *et al.*, Nucl. Fusion **53**, 113010 (2013).

[4] N. Winsor *et al.*, Phys. Fluids **11**, 2448 (1968).

[5] H. Sugama and T.-H. Watanabe, J. Plasma Phys. **72**, 825 (2006).

[6] R. Fisher, Nucl. Fusion **52**, 123015 (2012).

[7] D. Zarzoso *et al.*, Phys. Rev. Lett. **110**, 125002 (2013).

[8] G. Fu, Phys. Rev. Lett. **101**, 185002 (2008).

[9] H. Berk and T. Zhou, Nucl. Fusion **50**, 035007 (2010).

[10] Z. Qiu *et al.*, Plasma Phys. Control. Fusion **52**, 095003 (2010).

[11] Y. I. Kolesnichenko *et al.*, Plasma Phys. Control. Fusion **55**, 125007 (2013).

[12] L. Wang *et al.*, Phys. Plasmas **21**, 072511 (2014).

[13] D. Zarzoso *et al.*, Phys. Plasmas **19**, 022102 (2012).

[14] H. Wang and Y. Todo, Phys. Plasmas **20**, 012506 (2013).

[15] H. Wang *et al.*, Phys. Rev. Lett. **110**, 155006 (2013).

[16] D. Zarzoso *et al.*, Nucl. Fusion **54**, 103006 (2014).

[17] G. F. Chew *et al.*, Proc. R. Soc. Lond. A. Math. Phys. Sci. **236**, 112 (1956).

[18] Y. I. Kolesnichenko *et al.*, Plasma Phys. Control. Fusion **54**, 105001 (2012).

[19] R. Sgalla *et al.*, Phys. Lett. A **377**, 303 (2013).

[20] J. J. Ramos, Phys. Plasmas **10**, 3601 (2003).

[21] J. J. Ramos, Phys. Plasmas **12**, 052102 (2005).

[22] J.-B. Girardo *et al.*, Phys. Plasmas **21**, 092507 (2014).

[23] A. Hasegawa, Phys. Rev. Lett. **169**, 204 (1968).